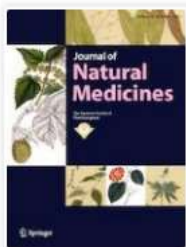




Journal of  
**Natural  
Medicines**



Springer



### Quality evaluation of *Angelicae acutilobae radix*: individual differences and localization of (*Z*)-ligustilide in *Angelica acutiloba* root

Yoshitomi Kudo, Hirokazu Ando & Yohei Sasaki

Original Paper | Published: 31 July 2020 | Pages: 1 - 10



### Characterization of metabolites in *Saposhnikovia divaricata* root from Mongolia

Zolboo Batsukh, Kazufumi Toume ... Katsuko Komatsu

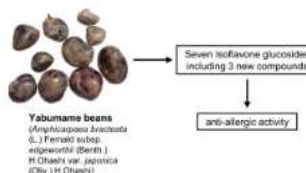
Original Paper | Published: 01 August 2020 | Pages: 11 - 27



### New isoflavone glucosides in yabumame (*Amphicarpaea bracteata* (L.) Fernald subsp. *edgeworthii* (Benth.) H. Ohashi var. *japonica* (Oliv.) H. Ohashi) and their effect on leukotriene B<sub>4</sub> production in mast cells

Lifeng Yang, Jyunichi Kirikoshi ... Hirofumi Arai

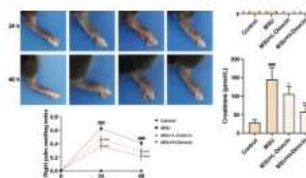
Original Paper | Published: 16 August 2020 | Pages: 28 - 36



### Preventive effect of dioscin against monosodium urate-mediated gouty arthritis through inhibiting inflammasome NLRP3 and TLR4/NF-κB signaling pathway activation: an in vivo and in vitro study

Jieru Han, Guangyu Shi ... Deyou Jiang

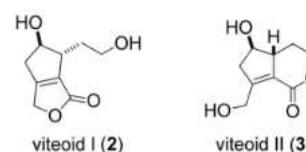
Original Paper | Published: 06 August 2020 | Pages: 37 - 47



### Iridoids isolated from *Vitidis Fructus* inhibit paclitaxel-induced mechanical allodynia in mice

Huanhuan Yu, Kazufumi Toume ... Katsuko Komatsu

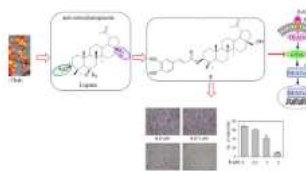
Original Paper | Published: 20 August 2020 | Pages: 48 - 55



### Triterpenoids from *Celastrus orbiculatus* Thunb. inhibit RANKL-induced osteoclast formation and bone resorption via c-Fos signaling

Thi Oanh Vu, Phuong Thao Tran ... Jeong Ah Kim

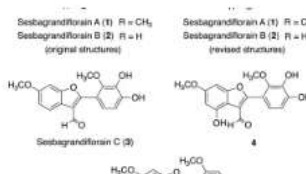
Original Paper | Published: 10 August 2020 | Pages: 56 - 65



### Structural revision of sesbagrandidiflorains A and B, and synthesis and biological evaluation of 6-methoxy-2-arylbenzofuran derivatives

Noviany Noviany, Arash Samadi ... Taifo Mahmud

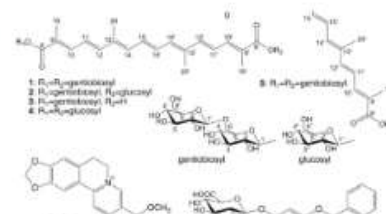
Original Paper | Published: 18 August 2020 | Pages: 66 - 75



## Solubility enhancement of berberine–baicalin complex by the constituents of Gardenia Fruit

Kazuki Okoshi, Yoshinori Uekusa ... Fumiyuki Kiuchi

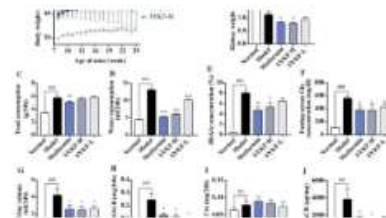
Original Paper | Published: 28 August 2020 | Pages: 76 - 83



## Shenyan Kangfu tablet alleviates diabetic kidney disease through attenuating inflammation and modulating the gut microbiota

Qian Chen, Dongwen Ren ... Tao Wang

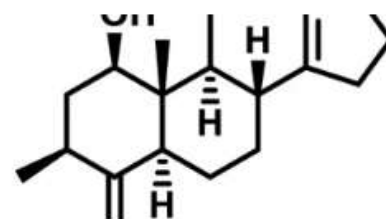
Original Paper | Published: 30 September 2020 | Pages: 84 - 98



## Acacienone, a terpenoid-like natural product having an unprecedented C20 framework isolated from *Acacia mangium* leaves

Yasumasa Hara, Yuichi Totsugi ... Masami Ishibashi

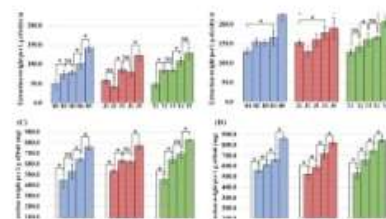
Original Paper | Published: 13 October 2020 | Pages: 99 - 104



## Changes in the extracted amounts and seasonally variable constituents of *Diospyros kaki* at different growth stages

Emi Katsumi, Naohiro Oshima ... Noriyasu Hada

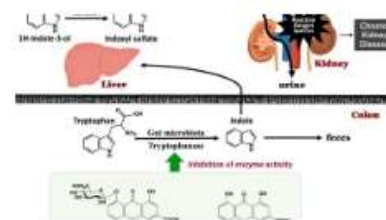
Original Paper | Published: 21 October 2020 | Pages: 105 - 115



## Antraquinone-containing compound in rhubarb prevents indole production via functional changes in gut microbiota

Kento Takayama, Shoji Maehara ... Nobuyuki Okamura

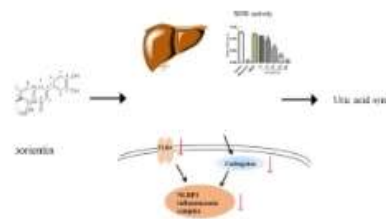
Original Paper | Published: 19 October 2020 | Pages: 116 - 128



## Isoorientin exerts a urate-lowering effect through inhibition of xanthine oxidase and regulation of the TLR4-NLRP3 inflammasome signaling pathway

Meng-Fei An, Ming-Yue Wang ... Jun Sheng

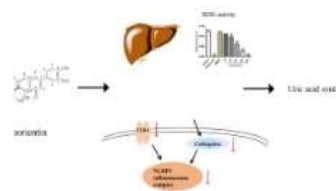
Original Paper | Published: 13 November 2020 | Pages: 129 - 141



## Isorientin exerts a urate-lowering effect through inhibition of xanthine oxidase and regulation of the TLR4-NLRP3 inflammasome signaling pathway

Meng-Fei An, Ming-Yue Wang ... Jun Sheng

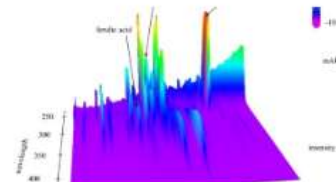
Original Paper | Published: 13 November 2020 | Pages: 129 - 141



## Oral administration of *Jumihaidokuto* inhibits UVB-induced skin damage and prostaglandin E2 production in HR-1 hairless mice

Kenta Murata, Manami Oyama ... Ryuji Takahashi

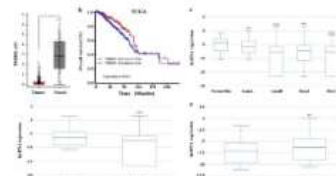
Original Paper | Open Access | Published: 17 November 2020 | Pages: 142 - 155



## Astragaloside IV inhibits cell proliferation and metastasis of breast cancer via promoting the long noncoding RNA TRHDE-AS1

Shufang Hu, Weihong Zheng & Li Jin

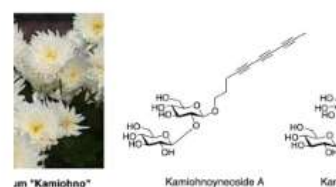
Original Paper | Published: 20 November 2020 | Pages: 156 - 166



## Kamiohnoynesides A and B, two new polyacetylene glycosides from flowers of edible Chrysanthemum "Kamiohno"

Shin-ichiro Kurimoto, Hiroki Fujita ... Takaaki Kubota

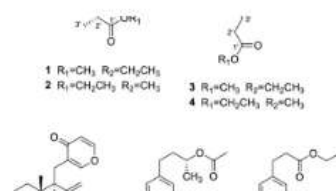
Note | Published: 17 August 2020 | Pages: 167 - 172



## Four new pyrrole alkaloids from the rhizomes of *Amomum koenigii*

Hong Yin, Chao Guo & Jin-Ming Gao

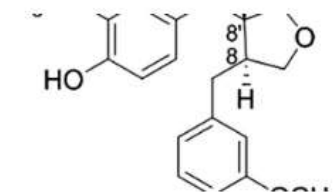
Note | Published: 21 October 2020 | Pages: 173 - 177



## Wikstromol from *Wikstroemia indica* induces apoptosis and suppresses migration of MDA-MB-231 cells via inhibiting PI3K/Akt pathway

Huankai Yao, Xiuli Zhang ... Qunli Wei

Note | Published: 31 August 2020 | Pages: 178 - 185



## PTP1B and $\alpha$ -glucosidase inhibitors from *Selaginella rolandi-principis* and their glucose uptake stimulation

Dinh-Tuan Nguyen, Dao-Cuong To ... Phi-Hung Nguyen

Note | Published: 14 September 2020 | Pages: 186 - 193



## Macrocarquinoids A–C, new meroterpenoids from *Sargassum macrocarpum*

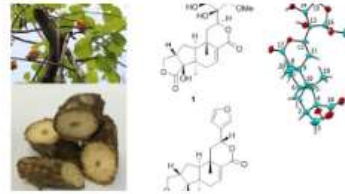
Hiromi Niwa, Shin-ichiro Kurimoto ... Mitsuhiko Sekiguchi

Note | Published: 24 September 2020 | Pages: 194 - 200



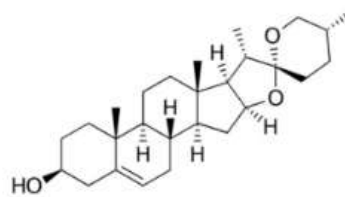
## Two new rearranged clerodane diterpenes from Thai *Tinospora baenzigeri*

Sujitra Hanthanong, Siwattra Choodej ... Khanitha Pudhom  
Note | Published: 24 September 2020 | Pages: 201 - 206



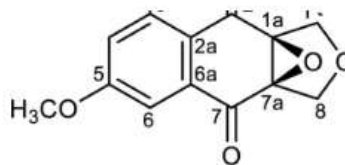
## Diosgenin content is a novel criterion to assess memory enhancement effect of yam extracts

Ximeng Yang, Kaori Nomoto & Chihiro Tohda  
Note | Published: 26 September 2020 | Pages: 207 - 216



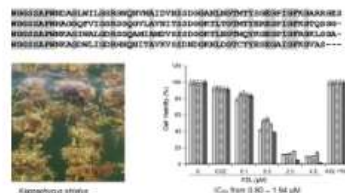
## Epoxyquinophomopsins A and B from endophytic fungus *Phomopsis* sp. and their activity against tyrosine kinase

Elvira Hermawati, Suzany D. Ellita ... Hayato Ishikawa  
Note | Published: 08 October 2020 | Pages: 217 - 222



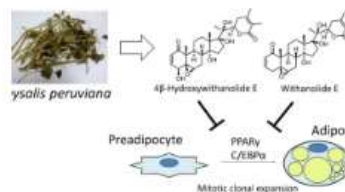
## Structure and anticancer activity of a new lectin from the cultivated red alga, *Kappaphycus striatus*

Le Dinh Hung & Phan Thi Hoai Trinh  
Note | Published: 06 October 2020 | Pages: 223 - 231



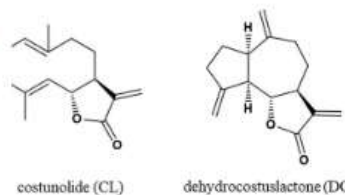
## 4 $\beta$ -Hydroxywithanolide E and withanolide E from *Physalis peruviana* L. inhibit adipocyte differentiation of 3T3-L1 cells through modulation of mitotic clonal expansion

Momochika Kumagai, Izumi Yoshida ... Yoshiki Morimoto  
Note | Published: 16 November 2020 | Pages: 232 - 239



## Costunolide and dehydrocostuslactone from *Saussurea lappa* root inhibit autophagy in hepatocellular carcinoma cells

Shinya Okubo, Tomoe Ohta ... Takuhiro Uto  
Note | Published: 06 November 2020 | Pages: 240 - 245



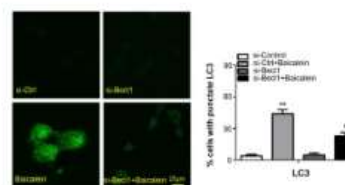
## Environmental and soil characteristics in *Ephedra* habitats of Uzbekistan

Motoyasu Minami, Fujii Taichi ... Takahisa Nakane  
Natural Resource Letter | Published: 22 October 2020 | Pages: 246 - 258




## Correction to: Inhibiting reactive oxygen species-dependent autophagy enhanced baicalein-induced apoptosis in oral squamous cell carcinoma

Bo Li, Mei Lu ... Mei Chen  
Correction | Published: 06 October 2020 | Pages: 259 - 259

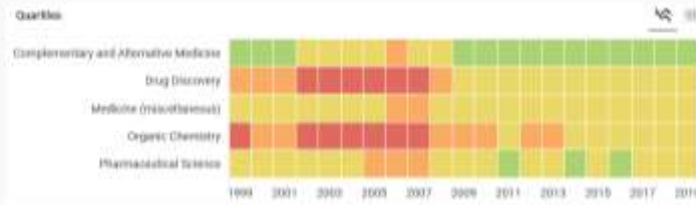


# Journal of Natural Medicines

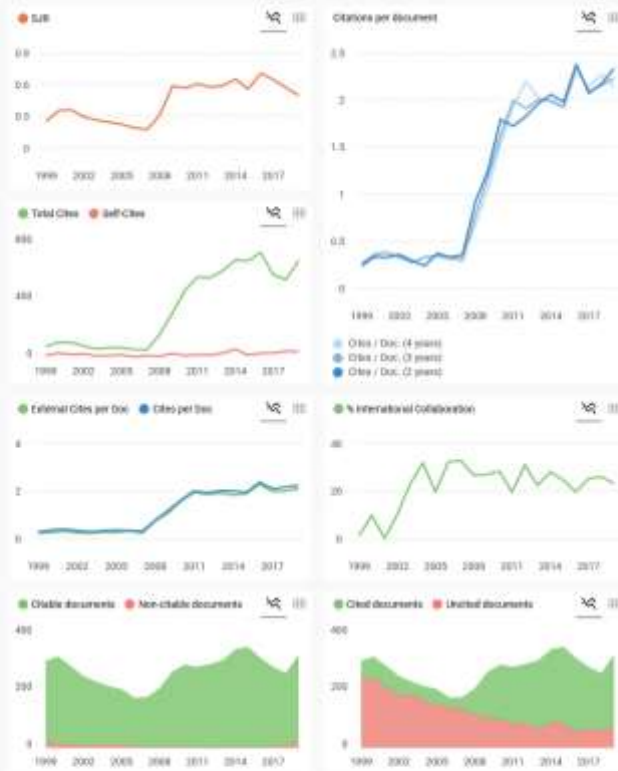
<b>COUNTRY</b> <a href="#">Germany</a> 	<b>SUBJECT AREA AND CATEGORY</b> <a href="#">Chemistry</a> <ul style="list-style-type: none"><li><a href="#">Organic Chemistry</a></li></ul> <a href="#">Medicine</a> <ul style="list-style-type: none"><li><a href="#">Complementary and Alternative Medicine</a></li><li><a href="#">Medicine (miscellaneous)</a></li></ul> <a href="#">Pharmacology, Toxicology and Pharmaceutics</a> <ul style="list-style-type: none"><li><a href="#">Drug Discovery</a></li><li><a href="#">Pharmaceutical Science</a></li></ul>	<b>PUBLISHER</b> <a href="#">Springer Verlag</a>
<b>H-INDEX</b> <b>41</b>	<b>PUBLICATION TYPE</b> <a href="#">Journals</a>	<b>ISSN</b> 13403443, 18610293
<b>COVERAGE</b> 2006-2020	<b>INFORMATION</b> <a href="#">Homepage</a> <a href="#">How to publish in this journal</a> <a href="mailto:mish@crife-uji">mish@crife-uji</a>	

## SCOPE

The Journal of Natural Medicines is an international journal publishing original research in naturally occurring medicines and their related foods and cosmetics. It covers: -chemistry of natural products -biochemistry of medicinal plants -pharmacology of natural products and herbs, including Kampo formulas and traditional herbs -botanical anatomy -cultivation of medicinal plants. The journal accepts Original Papers, Notes, Rapid Communications and Natural Resource Letters. Reviews and Mini-Reviews are generally invited.



FIND SIMILAR JOURNALS



Journal of Natural Medicines

Complementary and Alternative Medicine

Q1

0.49

powered by scimago.com

Show this widget in your own website

Just copy the code below and paste with your html code

<https://www.scimago.com>



NOTE

## Bisindole alkaloids from *Voacanga grandifolia* leaves

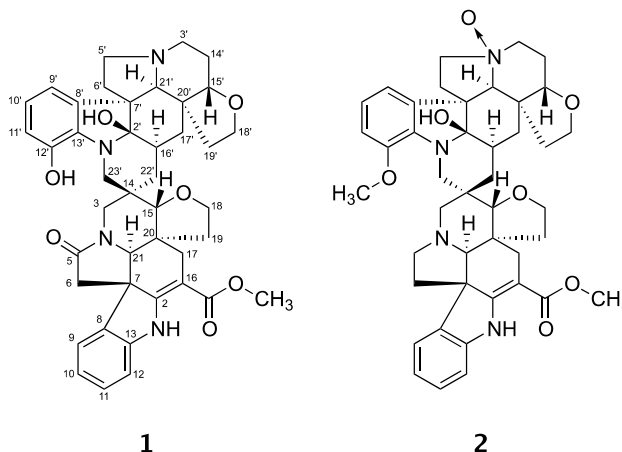
Alfarius Eko Nugroho<sup>1</sup> · Yurika Ono<sup>1</sup> · Eunji Jin<sup>1</sup> · Yusuke Hirasawa<sup>1</sup> · Toshio Kaneda<sup>1</sup> · Abdul Rahman<sup>1</sup> · Idha Kusumawati<sup>2</sup> · Takahiro Tougan<sup>3</sup> · Toshihiro Horii<sup>4</sup> · Noor Cholies Zaini<sup>2</sup> · Hiroshi Morita<sup>1</sup>

Received: 26 October 2020 / Accepted: 7 December 2020 / Published online: 19 January 2021  
© The Japanese Society of Pharmacognosy 2021

### Abstract

Two new bisindole alkaloids, 12'-*O*-demethyl-vobtusine-5-lactam and isovobtusine-*N*-oxide (**1** and **2**), were isolated from the leaves of *Voacanga grandifolia*, together with two known bisindole alkaloids. Their structures were elucidated on the basis of 1D and 2D NMR data. **1** and **2** showed potent antimalarial activity against *Plasmodium falciparum* 3D7 and very low cytotoxic activity against a human cell line, HepG2 cells.

### Graphical abstract



**Keywords** *Voacanga grandifolia* · Bisindole alkaloids · Apocynaceae · Antimalarial activity

**Supplementary Information** The online version contains supplementary material available at <https://doi.org/10.1007/s11418-020-01475-w>.

✉ Hiroshi Morita  
moritah@hoshi.ac.jp

<sup>1</sup> Faculty of Pharmaceutical Sciences, Hoshi University, Ebara 2-4-41 Shinagawa-ku, Tokyo 142-8501, Japan

<sup>2</sup> Faculty of Pharmacy, Airlangga University, Jalan Dharmawangsa Dalam, Surabaya 60286, Indonesia

<sup>3</sup> Research Center for Infectious Disease Control, Research Institute for Microbial Diseases, Osaka University, 3-1 Yamadaoka, Suita, Osaka 565-0871, Japan

<sup>4</sup> Department of Molecular Protozoology, Research Institute for Microbial Diseases, Osaka University, 3-1 Yamadaoka, Suita, Osaka 565-0871, Japan

### Introduction

*Voacanga* is a small genus of the Apocynaceae family consisting of 12 species. Species of this genus are distributed mainly in the tropical Africa and Malaysia, and have been reported to contain vobasine, eburnane, iboga, and aspidosperma type of monoterpene indole alkaloids [1]. Various activities have been reported for monoterpene indole alkaloids, such as cytotoxic activity [2–4], anti-melanogenesis [5], anti-plasmodial [6], and vasorelaxant activities [7]. In the search for new bioactive compounds from tropical plants [8–15], alkaloid constituents of *V. grandifolia* leaves were investigated and two new bisindole alkaloids, 12'-*O*-demethyl-vobtusine-5-lactam and isovobtusine-*N*-oxide (**1** and **2**,



Fig. 1), were isolated together with vobtusine-*N*-oxide [16], and vobtusine-3-lactam [17]. The isolation and structure elucidation of **1** and **2** consisting of bis-aspidosperma-type skeleton, from the leaves of *Voacanga grandifolia*, and their antimalarial activities are reported herein.

## Results and discussions

Compound **1**  $\{[\alpha]_D^{24} - 117.6^\circ (c 1.0, \text{MeOH})\}$  was isolated as an optically active, yellow amorphous solid. The molecular formula was determined by HRESIMS ( $m/z$  719.3453  $[\text{M} + \text{H}]^+$ ,  $\Delta + 0.8$  mmu) as  $\text{C}_{42}\text{H}_{46}\text{N}_4\text{O}_7$ , and the IR absorption at  $3340\text{ cm}^{-1}$  and  $1715\text{ cm}^{-1}$  indicated the presence of hydroxy and carbonyl groups, respectively. Analysis of the  $^1\text{H}$  and  $^{13}\text{C}$  NMR data (Table 1) and the HSQC spectrum of **1** revealed the presence of six  $\text{sp}^3$  quaternary carbons, five  $\text{sp}^3$  methines, fourteen  $\text{sp}^3$  methylenes, one methyl, seven  $\text{sp}^2$  methines, and nine  $\text{sp}^2$  quaternary carbons. Among them, two  $\text{sp}^3$  methines ( $\delta_{\text{C}} 63.6$ ;  $\delta_{\text{H}} 2.60$ ,  $\delta_{\text{C}} 64.9$ ;  $\delta_{\text{H}} 3.97$ ) and four  $\text{sp}^3$  methylenes ( $\delta_{\text{C}} 44.5$ ;  $\delta_{\text{H}} 2.85$  and  $4.16$ ,  $\delta_{\text{C}} 44.6$ ;  $\delta_{\text{H}} 3.13$  and  $4.82$ ,  $\delta_{\text{C}} 48.8$ ;  $\delta_{\text{H}} 2.29$  and  $2.84$ , and  $\delta_{\text{C}} 52.0$ ;  $\delta_{\text{H}} 2.21$  and  $3.02$ ) ascribed to those attached to a nitrogen atom.

The gross structure of **1** was elucidated by analysis of 2D NMR data including the  $^1\text{H}$ - $^1\text{H}$  COSY, TOCSY, HSQC, and HMBC spectra in  $\text{CDCl}_3$  (Fig. 2). The  $^1\text{H}$ - $^1\text{H}$  COSY spectrum revealed the connectivity of seven partial structures **a** (C-9'~C-11'), **b** (C-5'~C-6'), **c** (C-3', C-14'~C-15'), **d** (C-16'~C-17', C-22'), **e** (C-18'~C-19'), **f** (C-18~C-19), and **g** (C-9~C-12) as shown in Fig. 2. These partial structures were classified into two units, **a**~**e** and **f**~**g**.

The connectivity of partial structures **b** and **c** and C-21' through a nitrogen atom was revealed by the HMBC

correlations of H-5'b and H-21' to C-3' ( $\delta_{\text{C}} 48.8$ ). The HMBC correlations from H-18'a and H-19'a to C-15' ( $\delta_{\text{C}} 80.5$ ), H-14'a to C-20' ( $\delta_{\text{C}} 44.0$ ), and H-19'b to C-17' ( $\delta_{\text{C}} 32.6$ ) and C-21' ( $\delta_{\text{C}} 63.6$ ) established the connections among C-15', C-17', C-19', and C-21' through C-20'.

In addition, HMBC cross peaks of H-6'b to C-8' ( $\delta_{\text{C}} 134.9$ ), H-9' to C-21', H-21' to C-2' ( $\delta_{\text{C}} 93.5$ ) and C-6' ( $\delta_{\text{C}} 31.2$ ), and H-16' to C-7' ( $\delta_{\text{C}} 55.9$ ) revealed the connectivity between C-6', C-16', C-21', and an indoline ring. Then, the HMBC correlations of H-23'b and OH-12' to C-13' ( $\delta_{\text{C}} 138.2$ ), OH-12' to C-12' ( $\delta_{\text{C}} 139.8$ ), and H-22'a and H-23'a to C-2' suggested the presence of hydroxyl groups at C-2' and C-12' in the indoline ring. These NMR data were characteristic of an aspidosperma-type skeleton.

On the other hand, the similar aspidosperma-type skeleton with a methoxy carbonyl at C-16 and a double bond between C-2 and C-16 was suggested by the HMBC correlations in the units **f** and **g** as shown in Fig. 2. The connection of two indole alkaloids through C-14 was revealed by the HMBC correlations from H-23'a to C-14 ( $\delta_{\text{C}} 38.1$ ) and C-22' ( $\delta_{\text{C}} 35.2$ ) and from H-23'b to C-3 ( $\delta_{\text{C}} 44.5$ ) and C-15 ( $\delta_{\text{C}} 87.8$ ). In particular, the HMBC correlations of H-3a, H<sub>2</sub>-6 and H-21 to C-5 ( $\delta_{\text{C}} 172.6$ ) confirmed the presence of a carbonyl at C-5. These data suggested the structure of **1** as 12'-*O*-demethyl-vobtusine-5-lactam.

The relative configuration of each monoterpene indole unit in **1** was assigned by NOESY correlations as shown in computer-generated 3D drawing (Fig. 3). In **1a** (partial structures **a**~**e**), the NOESY correlations of H-21'/H-18'a and H-9', and H-15'/H-18'b and H-17'b suggested that both C-21' and C-15' should be *S*\* and C-7' and C-20' should be *R*\*. The relative configuration of C-2' ( $\delta_{\text{C}} 93.5$ ) was deduced to be *R*\* based on the similarity with the chemical shift ( $\delta_{\text{C}} 93.7$ ) of vobtusine [17]. Stereochemistry of H-16' was elucidated to be  $\alpha$ -oriented by  $^3J_{\text{H-16'/H-17'a}}$  (13.0 Hz) and  $^3J_{\text{H-16'/H-22'b}}$  (13.4 Hz), and the NOESY correlations in **1a**. In **1b** (partial structures **f**~**g**), H-15 is  $\beta$ -oriented and C-20 should be *R*\* by the NOESY correlations of H-21/H-18 and H-19a. Stereochemistry of a spiro carbon (C-14) in **1c** should be assigned as *R*\* by the NOESY correlations, suggesting that the diazaspiro [5.5] undecane ring took a chair-chair conformation, as shown in Fig. 3. Finally, the NOESY correlations and  $^1\text{H}$ - $^1\text{H}$  coupling constant values suggested the relative configuration of **1** to be, as shown in Fig. 1, the same as vobtusine-3-lactam.

Compound **2**  $\{[\alpha]_D^{24} - 123.6^\circ (c 1.0, \text{MeOH})\}$  was isolated as an optically active, yellow amorphous solid. The molecular formula was determined by HRESIMS ( $m/z$  735.3765  $[\text{M} + \text{H}]^+$ ,  $\Delta 0.7$  mmu) as  $\text{C}_{43}\text{H}_{50}\text{N}_4\text{O}_7$ , and the IR absorption at  $3340\text{ cm}^{-1}$  and  $1685\text{ cm}^{-1}$  indicated the presence of hydroxy and carbonyl groups, respectively. In addition, the  $^{13}\text{C}$  NMR data of **2** (Table 1) were similar to those of vobtusine-*N*-oxide and isovobtusine [16,17]. The

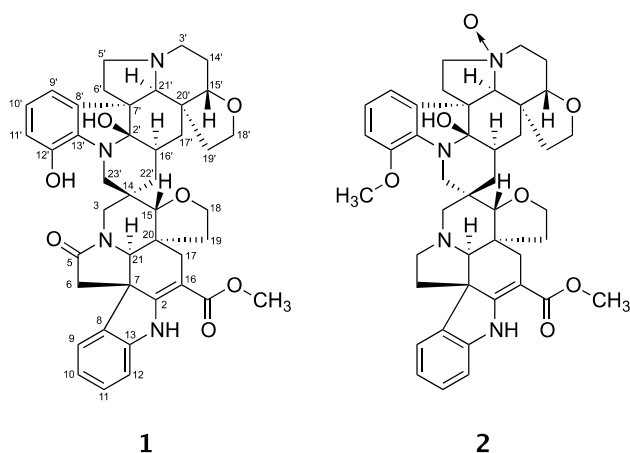


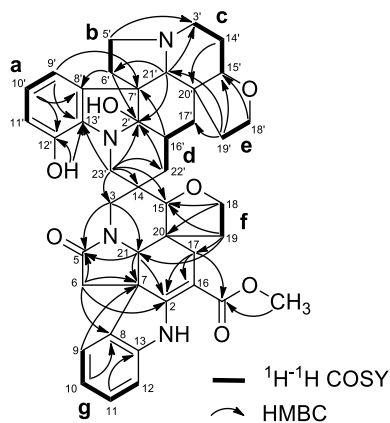
**Fig. 1** Structures of isolated compounds (**1** and **2**) from *Voacanga grandifolia*

**Table 1.**  $^1\text{H}$  (600 MHz) and  $^{13}\text{C}$  (150 MHz) NMR data of **1** and **2** in  $\text{CDCl}_3$ 

	<b>1</b>		<b>2</b>	
	$\delta_{\text{H}}$ (J, Hz)	$\delta_{\text{C}}$	$\delta_{\text{H}}$ (J, Hz)	$\delta_{\text{C}}$
2		164.4		167.5
3a	4.16 (1H, d, 13.0)	44.5	2.68 (1H, d, 10.8)	58.2
3b	2.85 (1H, d, 13.0)		2.64 (1H, d, 10.8)	
5a		172.6	2.89 (1H, m)	51.5
5b			2.74 (1H, m)	
6a	2.97 (1H, d, 18.0)	48.3	2.01 (1H, m)	44.4
6b	2.65 (1H, d, 18.0)		1.70 (1H, m)	
7		47.4		55.1
8		135.7		138.1
9	7.12 (1H, d, 7.5)	121.2	7.20 (1H, d, 7.2)	121.7
10	6.94 (1H, dd, 7.6, 7.5)	121.8	6.87 (1H, dd, 7.6, 7.2)	120.7
11	7.21 (1H, dd, 7.8, 7.6)	129	7.12 (1H, dd, 7.7, 7.6)	127.7
12	6.86 (1H, d, 7.8)	109.8	6.77 (1H, d, 7.7)	109.3
13		142.9		143
14		38.1		39.2
15	3.42 (1H, s)	87.8	3.17 (1H, s)	81.8
16		94		94.5
17a	2.52 (1H, s)	26.1	2.81 (1H, d, 13.8)	28.5
17b	2.52 (1H, s)		2.20 (1H, d, 13.8)	
18a	3.72 (1H, m)	63.9	3.65 (1H, m)	63.6
18b	3.72 (1H, m)		3.30 (1H, m)	
19a	1.56 (1H, m)	35.9	1.26 (1H, m)	35
19b	1.39 (1H, ddd, 13.0, 7.9, 4.8)		1.17 (1H, m)	
20		46.5		47.9
21	3.97 (1H, s)	64.9	2.83 (1H, s)	70
CO		168		168.4
OMe	3.80 (3H, s)	51.4	3.71 (3H, s)	51
2'		93.5		92.3
3'a	2.84 (1H, m)	48.8	3.45 (1H, m)	58.7
3'b	2.29 (1H, m)		3.45 (1H, m)	
5'a	3.02 (1H, m)	52	3.52 (1H, m)	67.2
5'b	2.21 (1H, m)		3.32 (1H, m)	
6'a	2.79 (1H, m)	31.2	3.58 (1H, m)	30.7
6'b	1.24 (1H, m)		1.36 (1H, m)	
7'		55.9		55.6
8'		134.9		133.6
9'	6.74 (1H, d, 7.3)	116	6.64 (1H, d, 7.6)	111.1
10'	6.61 (1H, dd, 7.3, 7.2)	119.1	6.62 (1H, dd, 7.6, 7.6)	118.1
11'	6.72 (1H, d, 7.2)	121.6	6.59 (1H, d, 7.6)	112.5
12'		139.8		146.3
13'		138.2		137.7
14'a	1.95 (1H, br d, 12.0)	25.8	2.92 (1H, m)	22.8
14'b	1.86 (1H, m)		2.01 (1H, m)	
15'	3.44 (1H, br s)	80.5	3.66 (1H, dd, 2.9, 2.9)	78.7
16'	1.87 (1H, m)	31.6	2.03 (1H, m)	33.9
17'a	1.78 (1H, dd, 13.0, 13.0)	32.6	2.56 (1H, dd, 12.5, 12.5)	33.7
17'b	0.86 (1H, br d, 13.0)		0.91 (1H, br d, 12.5)	
18'a	4.05 (1H, m)	65.4	3.98 (1H, m)	65
18'b	3.90 (1H, m)		3.90 (1H, m)	

**Table 1.** (continued)

	<b>1</b>		<b>2</b>	
	$\delta_{\text{H}}$ (J, Hz)	$\delta_{\text{C}}$	$\delta_{\text{H}}$ (J, Hz)	$\delta_{\text{C}}$
19'a	2.35 (1H, m)	36.5	2.48 (1H, ddd, 12.5, 8.1, 3.9)	39.7
19'b	1.52 (1H, m)		1.69 (1H, m)	
20'		44.0		45.4
21'	2.60 (1H, s)	63.6	3.56 (1H, s)	75.3
22'a	1.48 (1H, br d, 13.6)	35.2	2.00 (1H, m)	35
22'b	2.13 (1H, dd, 13.6, 13.4)		2.00 (1H, m)	
23'a	4.82 (1H, d, 14.5)	44.6	4.69 (1H, d, 14.1)	46.7
23'b	3.13 (1H, d, 14.5)		3.02 (1H, d, 14.1)	
12'-OH	6.22 (1H, s)			
12'-OMe			3.75 (3H, s)	54.9

**Fig. 2** Selected 2D NMR correlations of **1**

chemical shift differences between **2** and vobtusine-*N*-oxide (i.e. C-3, C-14, C-15, C-18, C-16', C-22' and C-23') suggested **2** to be the 14-*epi* derivative of vobtusine-*N*-oxide, isovobtusine-*N*-oxide, and the downfield shifts of signals ascribed to C-3', C-5' and C-21' in **2** relative to isovobtusine further supported this conclusion.

### Biological activity of **1** and **2**

The antimalarial activity and cytotoxic activity of **1** and **2** were evaluated in vitro. Against *P. falciparum* 3D7 strain, **1** and **2** showed potent antimalarial activity [Table 2: half-maximal (50%) inhibitory concentration ( $\text{IC}_{50}$ ) = 5.1 and 3.3  $\mu\text{M}$ , respectively]. Chloroquine was used as a positive control ( $\text{IC}_{50}$  = 0.026  $\mu\text{M}$ ). In contrast, the cytotoxic activity of both **1** and **2** was low [Table 2: half-maximal (50%) cytotoxic concentration ( $\text{CC}_{50}$ )  $\geq$  50  $\mu\text{M}$ ] against the human cell line, HepG2 cells.

## Experimental section

### General experimental procedures

Optical rotations were measured on a JASCO DIP-1000 polarimeter, UV spectra on a Shimadzu UVmini-1240 spectrophotometer, and IR spectra on a JASCO FT/IR-4100 spectrophotometer. High-resolution ESI MS were obtained on a JMS-T100LP (JEOL).  $^1\text{H}$  and 2D NMR spectra were measured on a 600 MHz spectrometer at 300 K, and  $^{13}\text{C}$  NMR spectra on a 150 MHz spectrometer. Residual solvent chemical shifts were used as internal standard,  $\delta_{\text{H}}$  7.26 and  $\delta_{\text{C}}$  77.0 for  $\text{CHCl}_3$ . Standard pulse sequences were used for the 2D NMR experiments.

### Material

The leaves of *V. grandiflora* were collected at the Purwodadi Botanical Garden in March 2008. The botanical identification was made by Ms. Sri Wuryanti, Purwodadi Botanical Garden. A voucher specimen has been deposited in the herbarium at Purwodadi Botanical Garden, Pasuruan, Indonesia.

### Extraction and isolation

Finely powdered leaves of *V. grandiflora* (400 g) were extracted with MeOH (1L  $\times$  3) at room temperature. The combined extracts were evaporated under reduced pressure to give a residue (30 g). The extract was dissolved in 3% aqueous tartaric acid (pH 2) and then partitioned with EtOAc. The aqueous layer was treated with  $\text{Na}_2\text{CO}_3$  to pH 9 and was partitioned successively by  $\text{CHCl}_3$  and *n*-BuOH. The  $\text{CHCl}_3$  soluble materials (3.9 g) was subjected to an LH-20 column ( $\text{CHCl}_3/\text{MeOH}$ , 1:1) to obtain ten fractions.

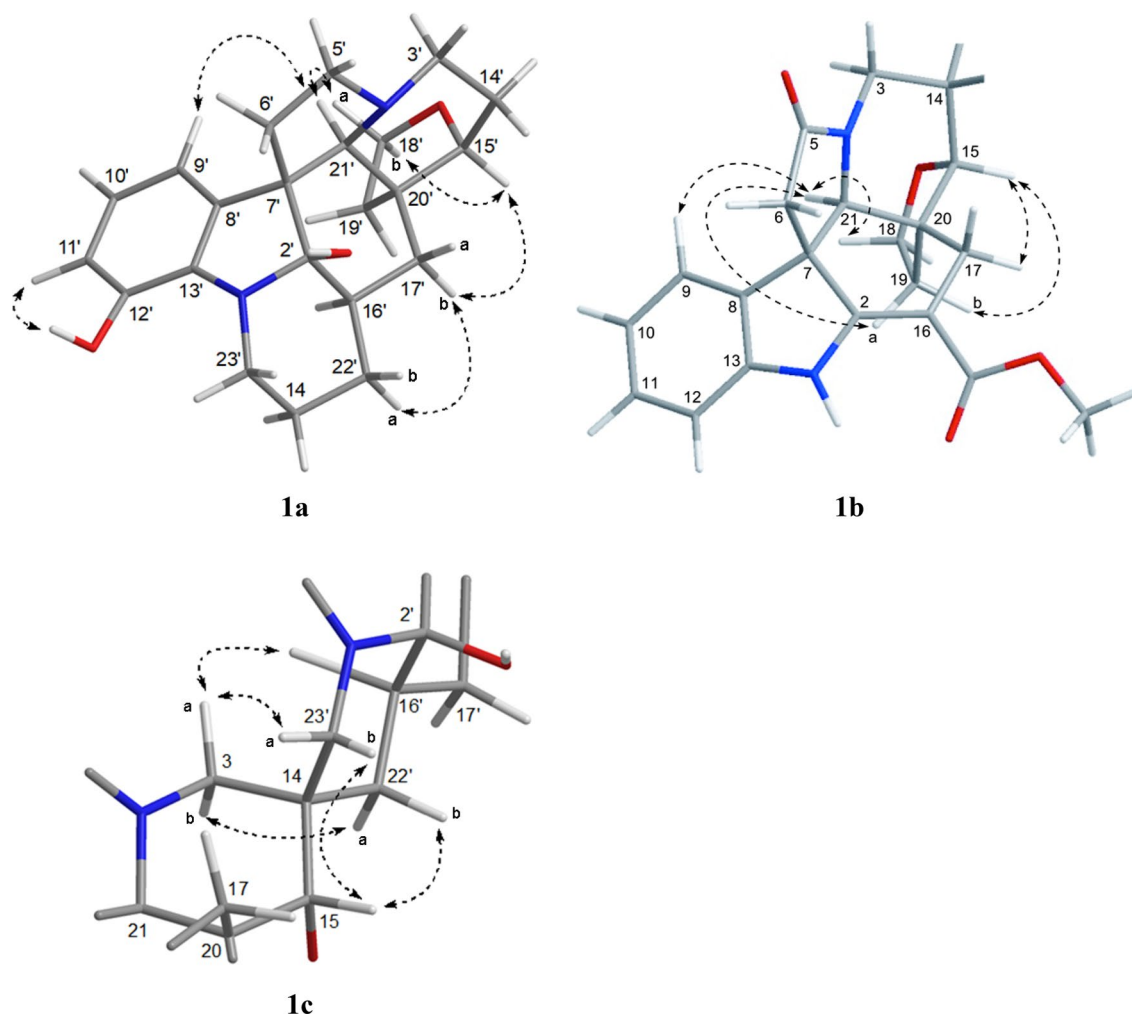


**Fig. 3** Selected NOESY correlations of **1**

**Table 2** Antimalarial and cytotoxic activities of **1** and **2** against *Plasmodium falciparum* 3D7

Compound	Antimalarial activity		Cytotoxic activity	
	IC <sub>50</sub> (μM)	CC <sub>50</sub> (μM)	IC <sub>50</sub> (μM)	CC <sub>50</sub> (μM)
<b>1</b>	5.1	> 50	> 50	> 50
<b>2</b>	3.3	> 50	> 50	> 50

Fraction 7 (360 mg) was fractionated by silica gel column chromatography (CHCl<sub>3</sub>/MeOH, 0:1 → 1:0), ODS column chromatography (MeOH/H<sub>2</sub>O) and RP-HPLC (Nacal tesque Cholesterol, 10×250 mm; 24% MeCN in 0.1% aqueous HCO<sub>2</sub>H; flow rate 3.5 mL/min; UV detection at 254 nm) to obtain **1** (1.5 mg, 0.0004%), **2** (1.5 mg, 0.0004%), vobtusine-*N*-oxide (1.9 mg, 0.0005%) [16], and vobtusine-3-lactam (0.8 mg, 0.0002%) [17].

**12'**-demethyl-vobtusine-5-lactam (**1**): Yellow amorphous solid; [α]<sub>D</sub> -117.6 (c 1.0, MeOH); IR (film) ν<sub>max</sub> 3340 and 1715 cm<sup>-1</sup>; UV/Vis λ<sub>max</sub> (MeOH) nm (log ε): 306 (3.57), 273 (3.84), 227 (4.41) and 206 (4.41) nm; ESIMS (pos.) *m/z* 719 (M + H)<sup>+</sup>; HRMS-ESI: *m/z* [M + H]<sup>+</sup> calcd for C<sub>42</sub>H<sub>47</sub>N<sub>4</sub>O<sub>7</sub>: 719.3445; found 719.3453.

Isovobtusine-*N*-oxide (**2**): Yellow amorphous solid; [α]<sub>D</sub> -123.6 (c 1.0, MeOH); IR (film) ν<sub>max</sub> 3370 and 1685 cm<sup>-1</sup>; UV/Vis λ<sub>max</sub> (MeOH) nm (log ε): 328 (4.22), 299 (4.16), 259 (3.93) and 220 (4.47) nm; ESIMS (pos.) *m/z* 735 (M + H)<sup>+</sup>; HRMS-ESI: *m/z* [M + H]<sup>+</sup> calcd for C<sub>43</sub>H<sub>51</sub>N<sub>4</sub>O<sub>7</sub>: 735.3758; found 735.3765.

### Parasite culture

*P. falciparum* laboratory strain 3D7 was obtained from Prof. Masatsugu Kimura (Osaka City University, Osaka, Japan). For the assessment of antimalarial activity of the compounds in vitro, the parasites were cultured in Roswell Park

Memorial Institute (RPMI) 1640 medium supplemented with 0.5 g/L L-glutamine, 5.96 g/L HEPES, 2 g/L sodium bicarbonate (NaHCO<sub>3</sub>), 50 mg/L hypoxanthine, 10 mg/L gentamicin, 10% heat-inactivated human serum, and red blood cells (RBCs) at a 3% hematocrit in an atmosphere of 5% CO<sub>2</sub>, 5% O<sub>2</sub>, and 90% N<sub>2</sub> at 37 °C as previously described [18]. Ring-form-infected RBCs were collected using the sorbitol synchronization technique [19]. Briefly, the cultured cells were collected by centrifugation at 840 g for 5 min at room temperature, suspended in a fivefold volume of 5% D-sorbitol (Nacalai Tesque, Kyoto, Japan) for 10 min at room temperature, and then they were washed twice with RPMI 1640 medium to remove the D-sorbitol. The utilization of blood samples of healthy Japanese volunteers for the parasite culture was approved by the institutional review committee of the Research Institute for Microbial Diseases (RIMD), Osaka University (approval number: 22–3).

### Antimalarial activity

Ring-form-synchronized parasites were cultured with compounds **1** and **2** at sequentially decreasing concentrations (50, 15, 5, 1.5, 0.5, 0.15, 0.05, and 0.015 μM) for 48 h for the flow cytometric analysis using an automated hematology analyzer, XN-30. The XN-30 analyzer was equipped with a prototype algorithm for cultured falciparum parasites [prototype; software version: 01–03, (build 16)] and used specific reagents (CELLPACK DCL, SULFOLYSER, Lysercell M, and Fluorocell M) (Sysmex, Kobe, Japan) [20,21]. Approximately 100 μL of the culture suspension diluted with 100 μL phosphate-buffered saline was added to a BD Microtainer MAP Microtube for Automated Process K2 EDTA 1.0 mg tube (Becton Dickinson and Co., Franklin Lakes, NJ, USA) and loaded onto the XN-30 analyzer with an auto-sampler as described in the instrument manual (Sysmex). The parasitemia shown as MI-RBC% was automatically reported [20]. Then 0.5% DMSO alone or containing 5 μM artemisinin used as the negative and positive controls, respectively. The growth inhibition (GI) rate was calculated from the MI-RBC% according to the following equation:

$$\text{GI}(\%) = 100 - \frac{(\text{test sample} - \text{positive control})}{(\text{negative control} - \text{positive control})} \times 100$$

The IC<sub>50</sub> was calculated from GI (%) using GraphPad Prism version 5.0 (GraphPad Prism Software, San Diego, CA, USA) [22].

### Cytotoxic activity

HepG2 (JCRB1054) cell line was obtained from the Japanese Collection of Research Bioresources (JCRB, Osaka,

Japan). The cells were cultured in Dulbecco's modified Eagle's medium [DMEM (1.0 g/L glucose) with L-glutamine and sodium pyruvate; Nacalai Tesque, Kyoto, Japan] supplemented with 10% (v/v) fetal bovine serum (FBS; Gibco-BRL, Grand Island, NY, USA) in a humidified incubator with 5% CO<sub>2</sub> at 37 °C. For the assay, the cells (5 × 10<sup>3</sup>/well) were seeded in a 96-well plate. **1** and **2** at gradually decreasing concentrations (50, 15, 5, 1.5, 0.5, 0.15, 0.05, and 0.015 μM) were added to the cell culture after 24 h and the cells were subsequently cultured for 48 h. Cell viability was measured using a Cell Counting Kit-8 (Dojindo, Kumamoto, Japan) according to the manufacturer's instructions. Briefly, 10 μL CCK-8 reagent was added to each well containing culture medium and incubated for 2 h under standard culture conditions. The absorbance of the sample was measured at 450 nm using a PowerWave HT microplate spectrophotometer (BioTek Instruments, Winooski, VT, USA). The cell viability was expressed as a percentage of the absorbance of the untreated control cells after subtracting the appropriate background intensity. The CC<sub>50</sub> was calculated from the cell viability using GraphPad Prism version 5.0.

**Acknowledgment** We thank Prof. Masatsugu Kimura (Osaka City University, Osaka, Japan) for the kind gift of the 3D7 strain. We also thank Mr. Yuji Toya and Dr. Kinya Uchihashi (Sysmex, Kobe, Japan) for the setting of the XN-30 analyzer and Ms. Toshie Ishisaka and Ms. Sawako Itagaki for their technical assistance. This work was supported by JSPS KAKENHI Grant Number JP19K07152 to MH and partially supported by Sysmex Corporation to TT.

### References

1. Macabeo APG, Alejandro GJD, Hallare AV, Vidar WS, Villaflores OB (2009) Phytochemical Survey and Pharmacological Activities of the Indole Alkaloids in the Genus *Voacanga* Thouars (Apocynaceae) - An Update. *Phcog Rev* 3:132-142
2. Hirasawa Y, Shoji T, Arai T, Nugroho AE, Deguchi J, Hosoya T, Uchiyama N, Goda Y, Awang K, Hadi AHA, Shiro M, Morita H (2010) Bisleuconothine a, an eburnane-aspidosperma bisindole alkaloid from *Leuconotis griffithii*. *Bioorg Med Chem Lett* 20:2021–2024
3. Haseo A, Nugroho AE, Hirasawa Y, Kaneda T, Shirota O, Rachman A, Kusumawati I, Zaini NC, Morita H (2015) A new indole alkaloids from *Voacanga grandifolia*. *Heterocycles* 90:601–606
4. Wong CP, Seki A, Horiguchi K, Shoji T, Arai T, Nugroho AE, Hirasawa Y, Sato F, Kaneda T, Morita H (2015) Bisleuconothine a induces autophagosome formation by interfering with AKT-mTOR signaling pathway. *J Nat Prod* 78:1656–1662
5. Koyama K, Hirasawa Y, Hosoya T, Hoe TC, Chan K-L, Morita H (2010) Alpnemines A-H, new anti-melanogenic indole alkaloids from *Alstonia pneumatophora*. *Bioorg Med Chem* 18:4415–4421
6. Nugroho AE, Sugai M, Hirasawa Y, Hosoya T, Awang K, Hadi AHA, Ekasari W, Widyawaruyanti A, Morita H (2011) New anti-plasmodial indole alkaloids from *Hunteria zeylanica*. *Bioorg Med Chem Lett* 21:3417–3419
7. Hirasawa Y, Hara M, Nugroho AE, Sugai M, Zaima K, Kawahara N, Goda Y, Awang K, Hadi AHA, Litaudon M, Morita H (2010) Bisnialaterines B and C, atropisomeric bisindole alkaloids from

- hunteria zeylanica*, showing vasorelaxant activity. J Org Chem 75:4218–4223
8. Nugroho AE, Hashimoto A, Wong CP, Yokoe H, Tsubuki M, Kaneda T, Hadi AHA, Morita H (2018) Ceramicines M-P from *Chisocheton ceramicus*: isolation and structure–activity relationship study. J Nat Med 72:64–72
  9. Nugroho AE, Inoue D, Wong CP, Hirasawa Y, Kaneda T, Shiota O, Hadi AHA, Morita H (2018) Reinereins A and B, new onocerane triterpenoids from *Reinwardtiidendron cinereum*. J Nat Med 72:588–592
  10. Kaneda T, Matsumoto M, Sotozono Y, Fukami S, Nugroho AE, Hirasawa Y, Hamid AHA, Morita H (2019) Cycloartane triterpenoid (23R, 24E)-23-acetoxymangiferonic acid inhibited proliferation and migration in B16–F10 melanoma via MITF downregulation caused by inhibition of both  $\beta$ -catenin and c-Raf–MEK1–ERK signaling axis. J Nat Med 73:47–58
  11. Tang Y, Nugroho AE, Hirasawa Y, Tougan T, Horii T, Hamid AHA, Morita H (2019) Leucophyllinines A and B, Bisindole alkaloids from *Leuconotis eugeniifolia*. J Nat Med 73:533–540
  12. Amelia P, Nugroho AE, Hirasawa Y, Kaneda T, Tougan T, Horii T, Morita H (2019) Indole alkaloids from *Tabernaemontana macrocarpa* Jack. J Nat Med 73:820–825
  13. Hirasawa Y, Dai X, Deguchi J, Hatano S, Ohtsuka R, Nugroho AE, Kaneda T, Morita H (2019) New Vasorelaxant Indole Alkaloids, Taberniacins A and B, from *Tabernaemontana divaricata*. J Nat Med 73:627–632
  14. Prema WCP, Awouafack MD, Nugroho AE, Win YY, Win NN, Ngwe H, Morita H, Morita H (2019) Two new quassinoids and other constituents from the *Picrasma javanica* wood and their biological activities. J Nat Med 73:589–596
  15. Prema WCP, Kodama T, Nugroho AE, El-Desoky AH, Awouafack MD, Win YY, Ngwe H, Abe I, Morita H, Morita H (2020) Three new quassinoids isolated from the wood of *Picrasma javanica* and their anti-Vpr activities. J Nat Med 74:571–578
  16. Agwada VC, Naranjo J, Hesse M, Schmid H, Rolland Y, Kunesch N, Poisson J, Chatterjee A (1977) Die struktur des bisindolalkaloides amatain (= grandifolin, subsessilin). Helv Chim Acta 60:2830–2853
  17. Rolland Y, Kunesch N, Poisson J, Hagaman EW, Schell FM, Wenkert E (1976) *Voacanga* alkaloids. 16. Carbon-13 nuclear magnetic resonance spectroscopy of naturally occurring substances. 43. Carbon-13 nuclear magnetic resonance analysis of bis-indoline alkaloids of two *Voacanga* species. J Org Chem 41:3270–3275
  18. Trager W, Jensen JB (1976) Human malaria parasites in continuous culture. Science 193:673–675
  19. Lambros C, Vanderberg JP (1979) Synchronization of *Plasmodium falciparum* erythrocytic stages in culture. J Parasitol 65:418–420
  20. Tougan T, Suzuki Y, Itagaki S, Izuka M, Toya Y, Uchihashi K, Horii T (2018) An automated haematology analyzer XN-30 distinguishes developmental stages of falciparum malaria parasite cultured in vitro. Malar J 17:59
  21. Toya T, Tougan T, Horii T, Uchihashi K (2021) Lysercell M enhances the detection of stage-specific Plasmodium-infected red blood cells in the automated hematology analyzer XN-31 prototype. Parasitol Int 80:102206. <https://pubmed.ncbi.nlm.nih.gov/33049417/>
  22. Tougan T, Toya Y, Uchihashi K, Horii T (2019) Application of the automated haematology analyzer XN-30 for discovery and development of anti-malarial drugs. Malar J 18:8

**Publisher's Note** Springer Nature remains neutral with regard to jurisdictional claims in published maps and institutional affiliations.